Supporting Information for

Tetradentate halogen bonding macrocyclic anion receptor inspired by the "Texas-sized" molecular box

Tian Zhao,[a] Vincent M. Lynch,[a] Jonathan L. Sessler[a,*]

[a] Department of Chemistry, The University of Texas at Austin, 105 East 24th, Street-Stop A5300, Austin, Texas 78712-1224, United States

* Corresponding author: Jonathan L. Sessler (E-mail: sessler@cm.utexas.edu)

Table of contents

1.General information

All solvents and chemicals used were purchased from Aldrich, TCI, and Acros and used without further purification. TLC analyses were carried out using Sorbent Technologies silica gel (200 mm) sheets. Column chromatography was performed on Sorbent silica gel 60 (40–63 mm). NMR spectra were recorded on a Agilent MR 400 instrument. The NMR spectra were referenced to solvent residue peaks and the spectroscopic solvents were purchased from Cambridge Isotope Laboratories and Aldrich. Electrospray ionization (ESI) mass spectra were recorded on a VG AutoSpec apparatus. X-ray crystallographic analyses were carried out on either a Rigaku AFC12 diffractometer equipped with a Saturn 724+ CCD or an Agilent Technologies SuperNova Dual Source diffractometer using a μ-focus Cu Kα radiation source (λ = 1.5418 Å) with collimating mirror monochromators. A graphite monochromator and MoKα radiation were used. Further details of the structures and their refinement is given in a later section.

Note: Many of the intermediates and products contain azide or triazole moieties, or both. Due to their potential thermal instability all manipulations involving such species were carried out at or below room temperature.

2.Synthesis and characterization

2.1 Synthesis of **1**

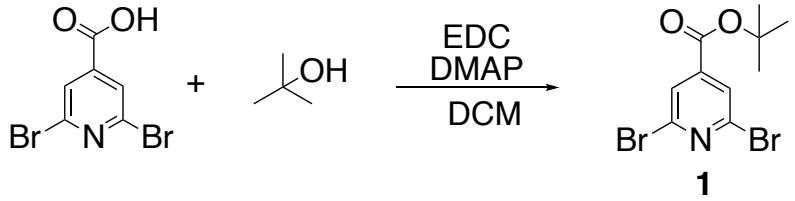

1

Precursor **1** was synthesized using a modification of a literature report.[S1] Briefly, 2,6-dibromopyridine-4-carboxylic acid (5.6 g, 20 mmol), EDC·HCl (7.67 g, 40 mmol) and dimethylaminopyridine (DMAP) (0.48 g, 4 mmol) were dissolved in dry dichloromethane (DCM) (70 ml). *tert*-Butyl alcohol (3.80 ml, 40 mmol) was then added to the mixture. The reaction was stirred at rt for 24 h and then washed with water and brine. The organic layer was separated, dried over $MgSO_4$ and evaporated under vacuum. The residue was purified by column chromatography (1:2 CH_2Cl_2/hexanes) to give **1** (5.97 g, 90%) as a white solid. ^{1}H NMR ($CDCl_3$, 400 MHz) δ (ppm): 7.90 (s, 2H), 1.58 (s, 9H). ^{13}C NMR ($CDCl_3$, 100 MHz) δ (ppm): 143.48, 141.31, 126.66, 83.91, 27.93. HRMS (ESI^+) *m/z* $[M+H]^+$: Calcd for $C_{10}H_{12}Br_2NO_2$ 335.9229, found: 335.9233.

2.2 Synthesis of **2**

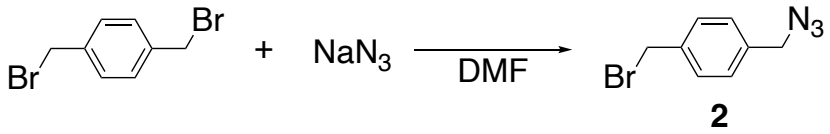

2

In accord with a literature report,[S2] α,α′-dibromo-*p*-xylene (6.72 g, 25.4 mmol) and sodium azide (1.61 g, 25.4 mmol) were dissolved in dimethylformamide (DMF) (30 mL). The reaction was stirred at room temperature overnight. Water (100 mL) was then added to quench the reaction and the mixture was extracted with DCM (3 × 100 mL). The combined organic layer was then washed with water several times to remove residual DMF. After evaporation of the volatiles, the crude product was purified by column chromatography (6:1 hexanes/CH_2Cl_2) to give **2** (2.30 g, 10.2 mmol, 45%) as a white solid. ^{1}H NMR ($CDCl_3$, 400 MHz) δ (ppm): 7.42 (d, J = 8.1 Hz, 2H), 7.30 (d, J = 8.2 Hz, 2H), 4.50 (s, 2H), 4.34 (s, 2H). ^{13}C NMR ($CDCl_3$, 100 MHz) δ (ppm): 137.9, 135.7, 129.5, 128.6, 54.4, 32.9. HRMS (CI^+) *m/z* $[M]^+$: Calcd for $C_8H_8BrN_3$ 224.9902, found: 224.9900.

2.3 Synthesis of **3**

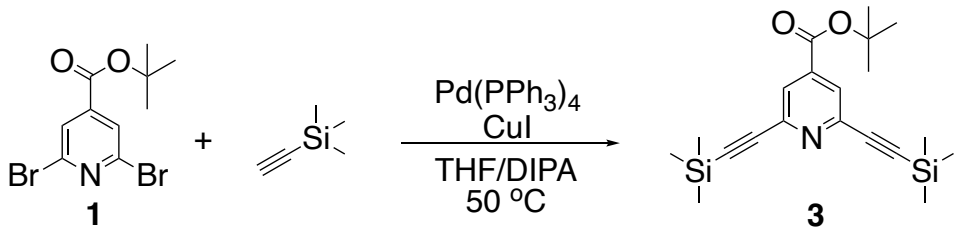

1 **3**

Precursor **1** (6.12 g, 18.16 mmol), CuI (340 mg, 1.82 mmol) and $Pd(PPh_3)_4$ (2.10 g, 1.82 mmol) were dissolved in 120 ml of a 1:1 (v/v) mixture of tetrahydrofuran (THF) and diisopropylamine. The solution was purged with N_2 gas for 20 minutes. Trimethylsilylacetylene (6.5 ml, 45.4 mmol) was then added using a syringe. The reaction was stirred at 50 °C for 8 h. After the volatiles were removed under reduced pressure, the residue was purified by column chromatography (20:1 hexanes/ethyl acetate) to give **3** (5.69 g, 84%) as a bright yellow solid. ^{1}H NMR ($CDCl_3$, 400 MHz) δ (ppm): 7.82 (s, 2H), 1.59 (s, 9H), 0.25 (s, 18H). ^{13}C NMR ($CDCl_3$, 100 MHz) δ (ppm): 162.90, 144.00, 139.95, 125.82, 102.60, 96.54, 83.07, 28.00, –0.40. HRMS (ESI^+) *m/z* $[M+H]^+$: Calcd for $C_{20}H_{30}NO_2Si_2$ 372.1810, found: 372.1824.

2.4 Synthesis of **4**

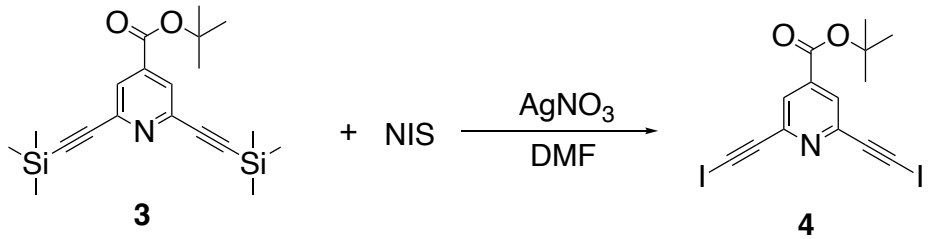

3 **4**

According to a modified literature procedure,[S3] intermediate **3** (1.5 g, 4.04 mmol), $AgNO_3$ (100 mg, 0.6 mmol) and N-iodosuccinimide (NIS) (1.98 g, 8.8 mmol) were dissolved in dry DMF (30

ml). The mixture was stirred in darkness at room temperature overnight. Subsequently, the solution was partitioned with water (100 ml) and DCM (100 ml). The organic phase was separated off, washed with water a few more times and dried over $MgSO_4$. This organic solution was then concentrated under vacuum and the resulting crude material purified by column chromatography over silica gel (4:1 hexanes/ethyl acetate) to give **4** as a dark red powder (1.73 g, 89%). ^{1}H NMR ($CDCl_3$, 400 MHz) δ (ppm): 7.79 (s, 2H), 1.57 (s, 9H). ^{13}C NMR ($CDCl_3$, 100 MHz) δ (ppm): 143.83, 126.31, 92.97, 83.29, 27.99, 12.25. HRMS (CI^+) *m/z* $[M]^+$: Calcd for $C_{14}H_{11}NO_2I_2$ 478.8879, found: 478.8880.

2.5 Synthesis of **5**

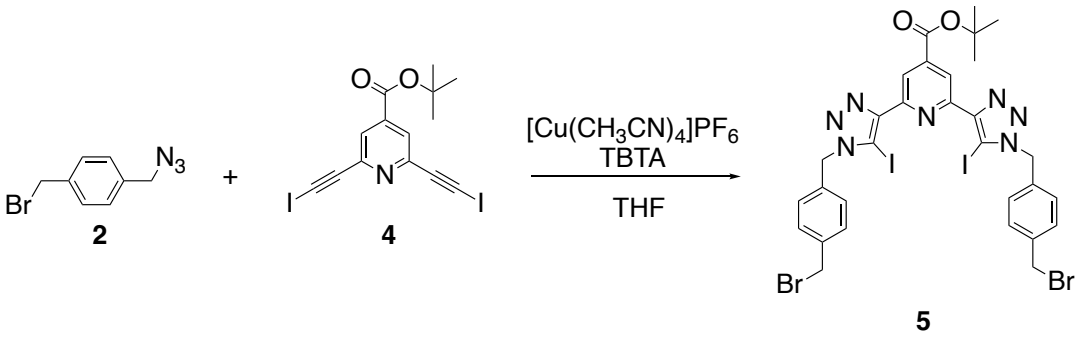

Intermediates **2** (742.5 mg, 3.3 mmol) and **4** (632.4 mg, 1.32 mmol) were added to dry THF (40 mL). The mixture was purged with N_2 gas. Cu[$(MeCN)_4$]PF_6 (50 mg, 0.132 mmol) and tris[(1-benzyl-1*H*-1,2,3-triazol-4-yl)methyl]amine (TBTA) (70 mg, 0.132 mmol) were then added to the mixture. The reaction was stirred at room temperature overnight protected from light. Subsequently, the reaction mixture was concentrated under vacuum and partitioned between a Na_2EDTA solution (100 ml) and DCM (100 ml). The organic phase was collected and concentrated under vacuum. The residue was purified by column chromatography (2:1 hexanes/ ethyl acetate) over silica gel to give **5** as a pale yellow solid (880 mg, 72%). ^{1}H NMR (DMSO-d_6, 400 MHz) δ (ppm): 8.35 (s, 2H), 7.12-7.55 (m, 8H), 5.77 (s, 4H), 4.69 (s, 4H), 1.61 (s, 9H). ^{13}C NMR (DMSO-d_6, 100 MHz) δ (ppm):138.37, 135.73, 130.20, 128.22, 34.35, 28.07. HRMS (ESI^+) *m/z* $[M+H]^+$: Calcd for $C_{30}H_{28}Br_2I_2N_7O_2$ 929.8755, found: 929.8732.

2.6 Synthesis of **6** & Ibox

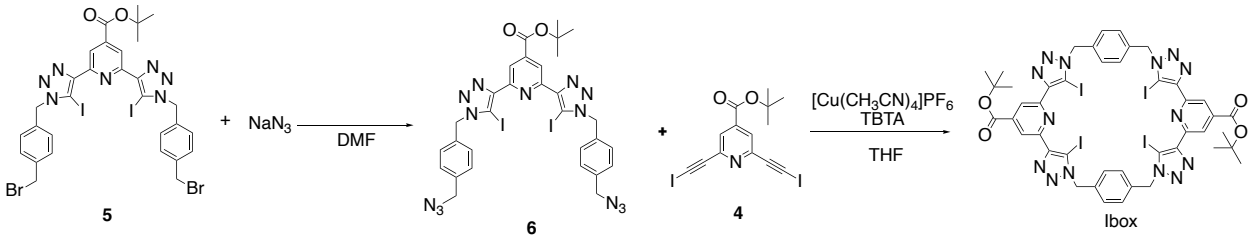

Intermediate **5** (880 mg, 0.947 mmol) and NaN_3 (154 mg, 2.37 mmol) were dissolved in DMF (60 ml). The mixture was stirred at room temperature protected from the light for 24 h. Then, water (300 mL) was added to quench the reaction, which was extracted with DCM (100 ml).

The organic layer was washed with water a few more times and dried over Na_2SO_4 before the volatiles were removed under vacuum to give crude **6** in essentially quantitative yield. This material was used without further purification. Here, $Cu[(MeCN)_4]PF_6$ (7.9 mg, 0.021mmol) and TBTA (11 mg, 0.021 mmol) were dissolved in dry THF (100 ml) under an N_2 atmosphere (referred to as the catalyst solution). Bis-azide **6** (178 mg, 0.209 mmol) and diiodide **4** (100 mg, 0.209 mmol) were dissolved in 10 ml dry THF and added to the catalyst solution over the course of 10 h by means of a syringe pump. The reaction mixture was stirred for another 48 h in the dark. Subsequently, the reaction mixture was concentrated under vacuum and partitioned between a Na_2EDTA solution (100 ml) and DCM (100 ml). The organic phase was separated and concentrated under reduced pressure. The residue was purified by column chromatography over silica gel (1:1 hexane/ethyl acetate) to give the Ibox in 60% isolated yield. ^1H NMR ($CDCl_3$, 400 MHz) δ (ppm): 8.56 (s, 4H), 7.18 (s, 8H), 5.68 (s, 8H), 1.62 (s, 18H). Due to solubility issues, a clean ^{13}C NMR spectrum could not be obtained. HRMS (ESI^+) *m/z* $[M+2H]^{2+}$: Calcd for $C_{44}H_{40}I_4N_{14}O_4$ 667.9762, found: 667.9778. This product was also characterized by means of a single crystal X-ray diffraction analysis.

2.7 Characterization data

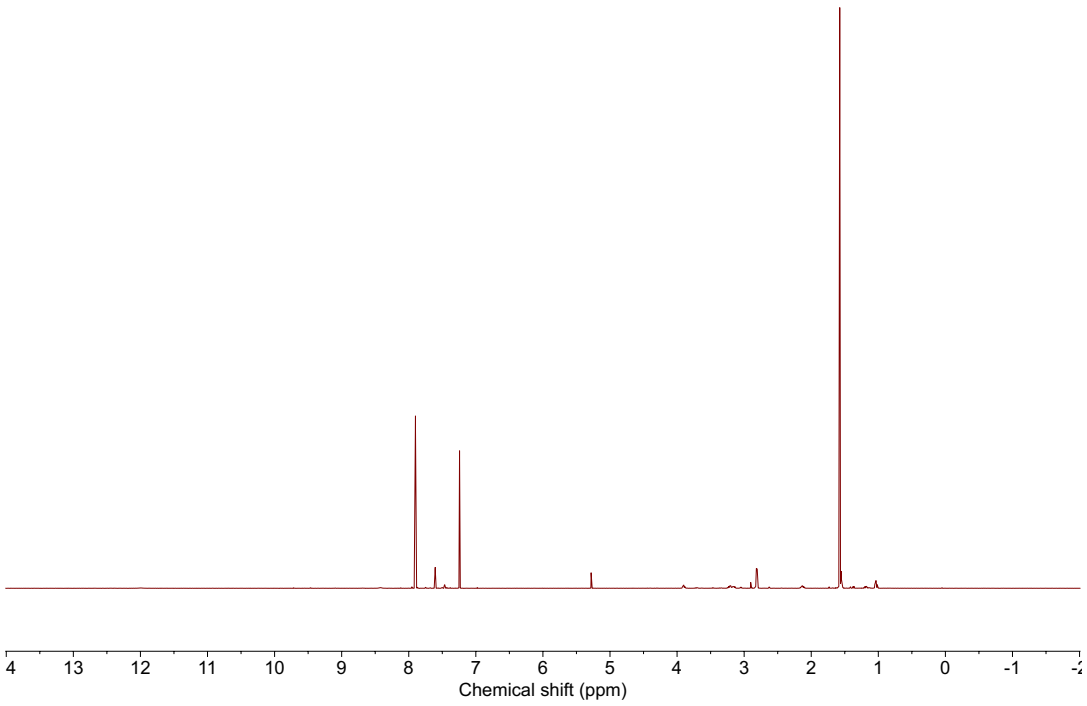

Fig. S1. ^1H NMR spectrum of compound **1** recorded in $CDCl_3$.

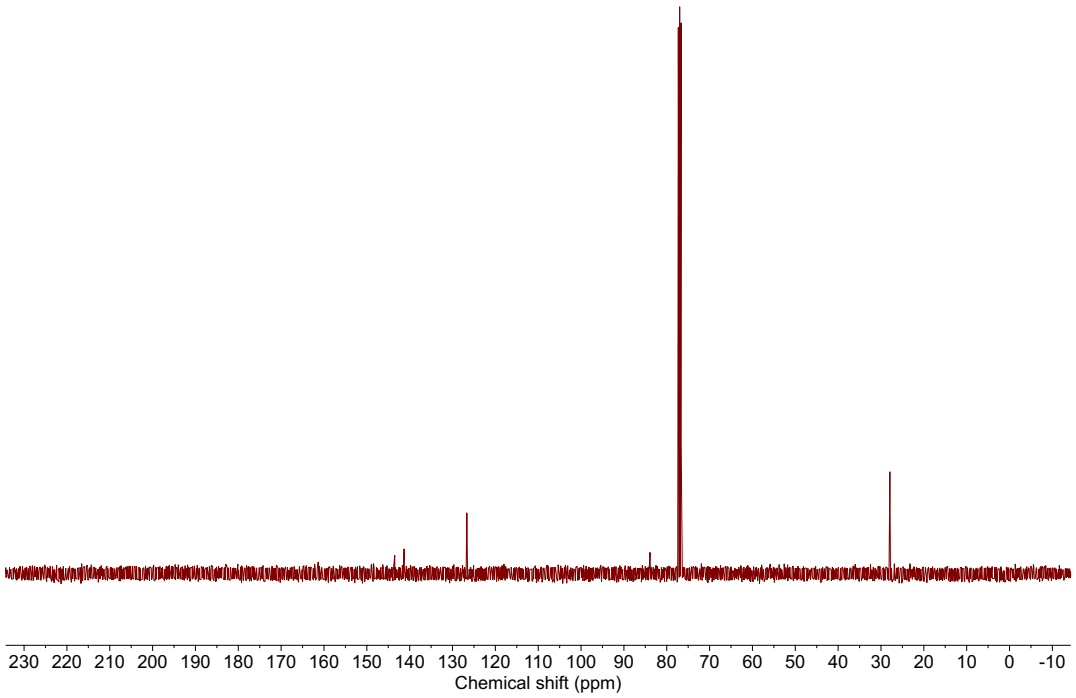

Fig. S2. ^{13}C NMR spectrum of compound **1** recorded in $CDCl_3$.

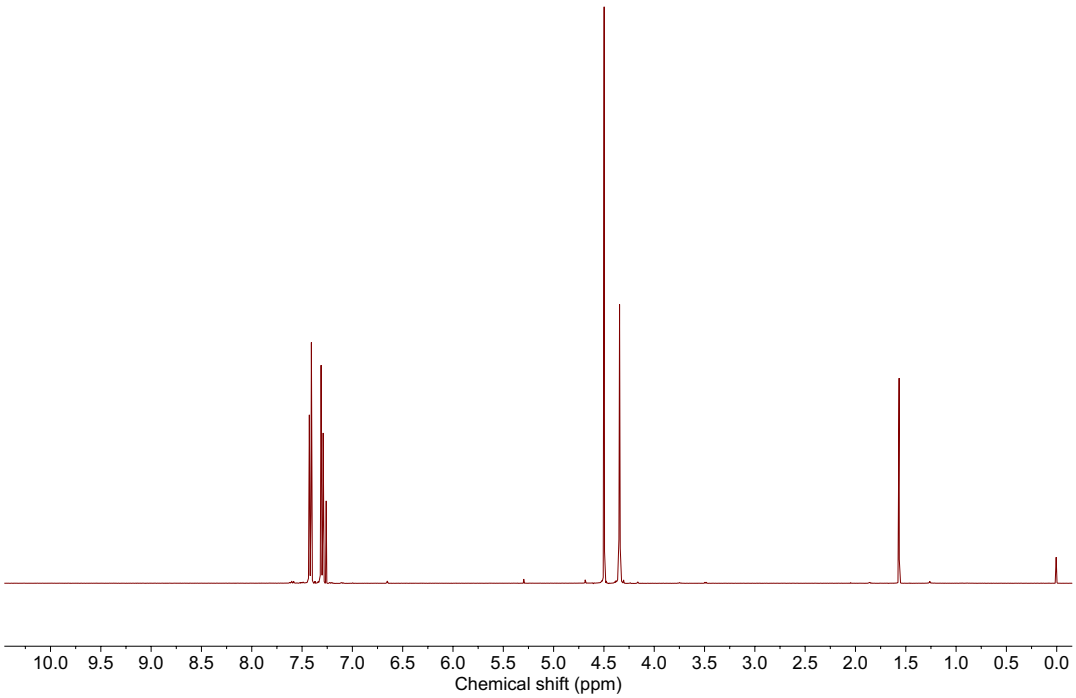

Fig. S3. ^{1}H NMR spectrum of compound **2** recorded in $CDCl_3$.

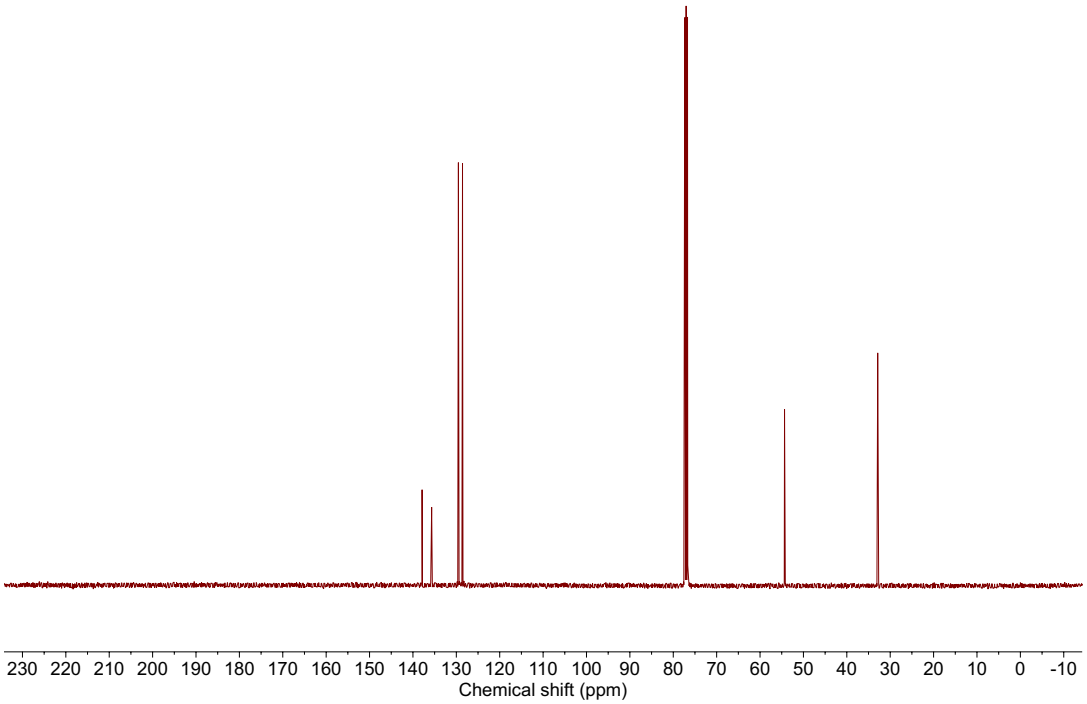

Fig. S4. ^{13}C NMR spectrum of compound **2** recorded in $CDCl_3$.

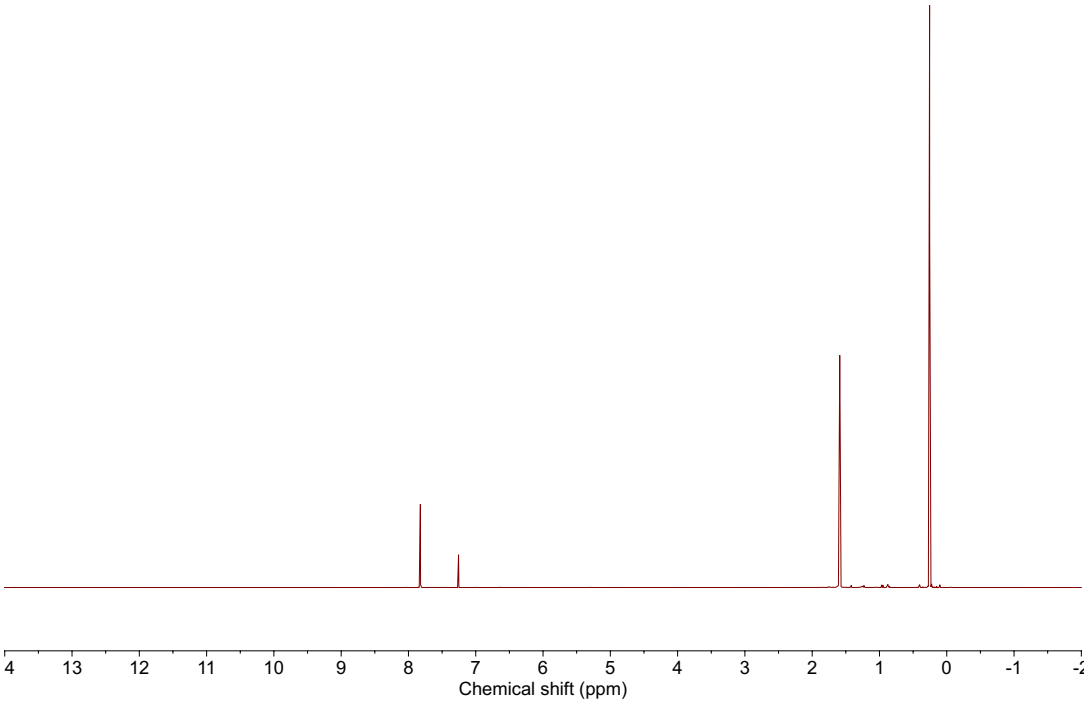

Fig. S5. ^{1}H NMR spectrum of compound **3** recorded in $CDCl_3$.

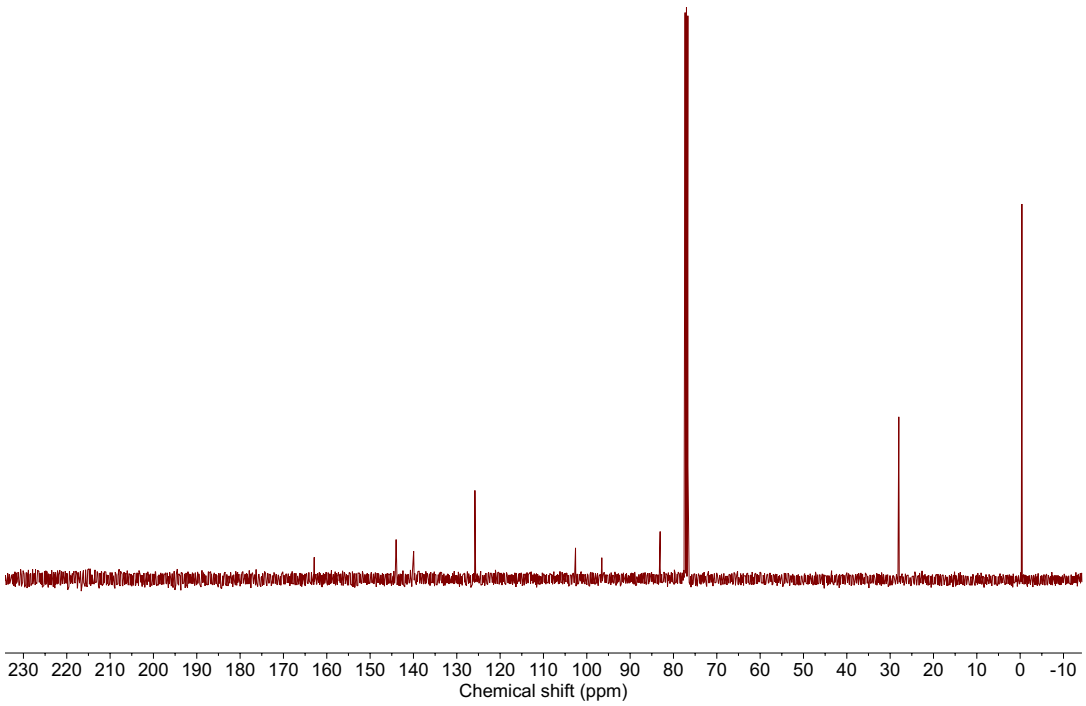

Fig. S6. ^{13}C NMR spectrum of compound **3** recorded in $CDCl_3$.

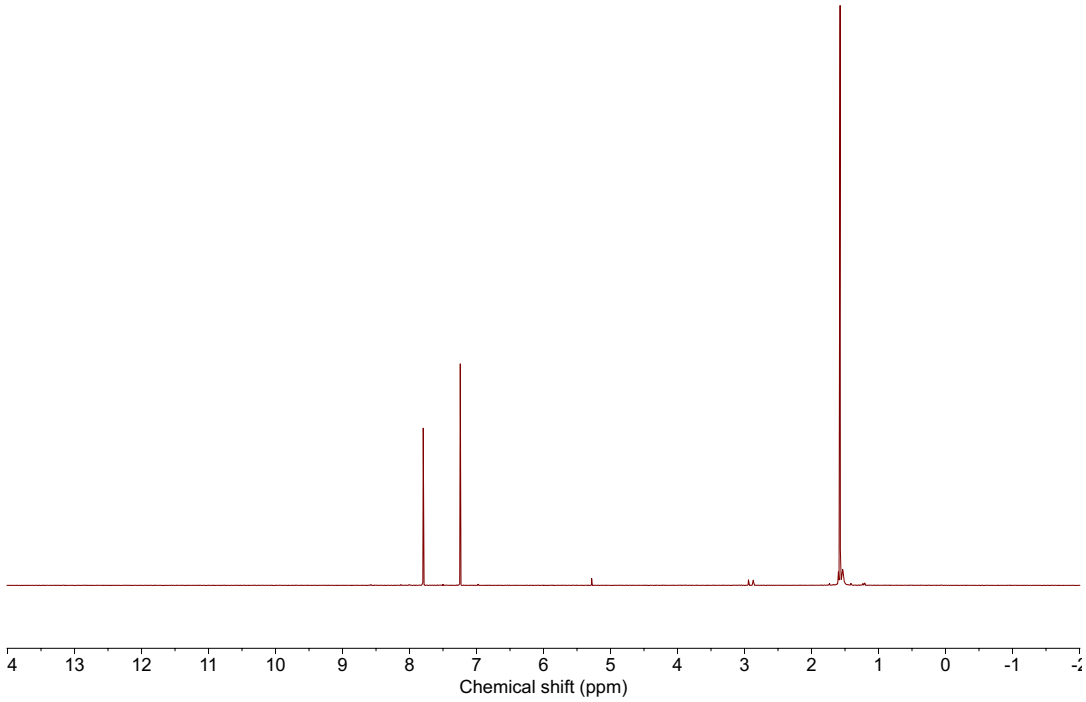

Fig. S7. ^{1}H NMR spectrum of compound **4** recorded in $CDCl_3$.

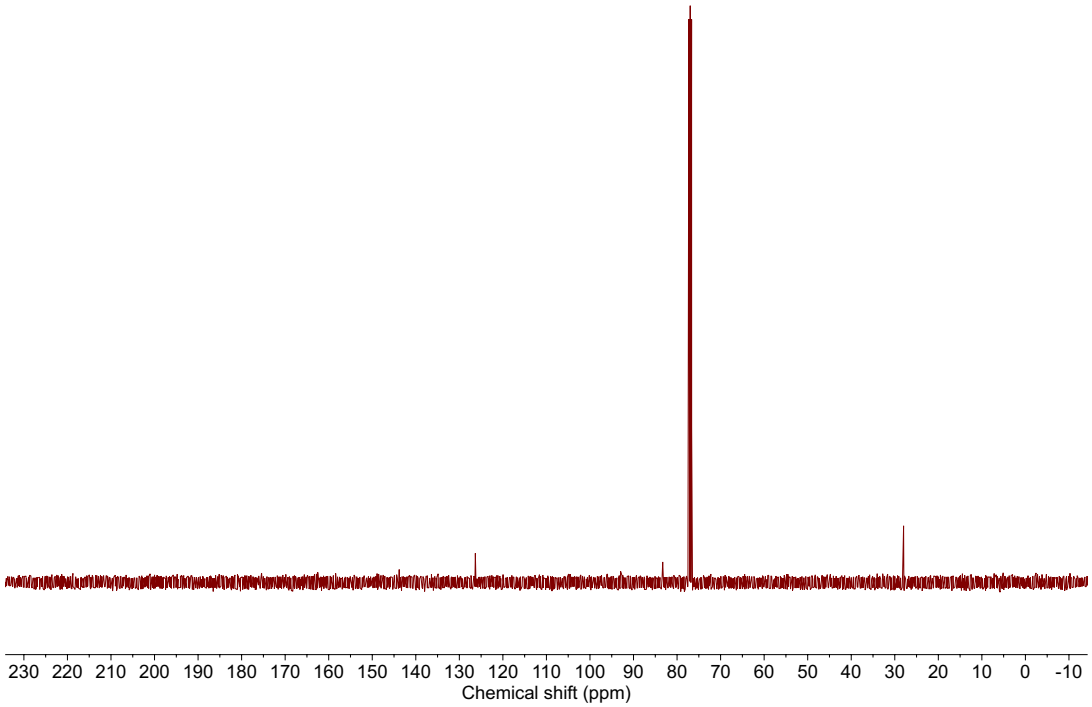

Fig. S8. ^{13}C NMR spectrum of compound **4** recorded in $CDCl_3$.

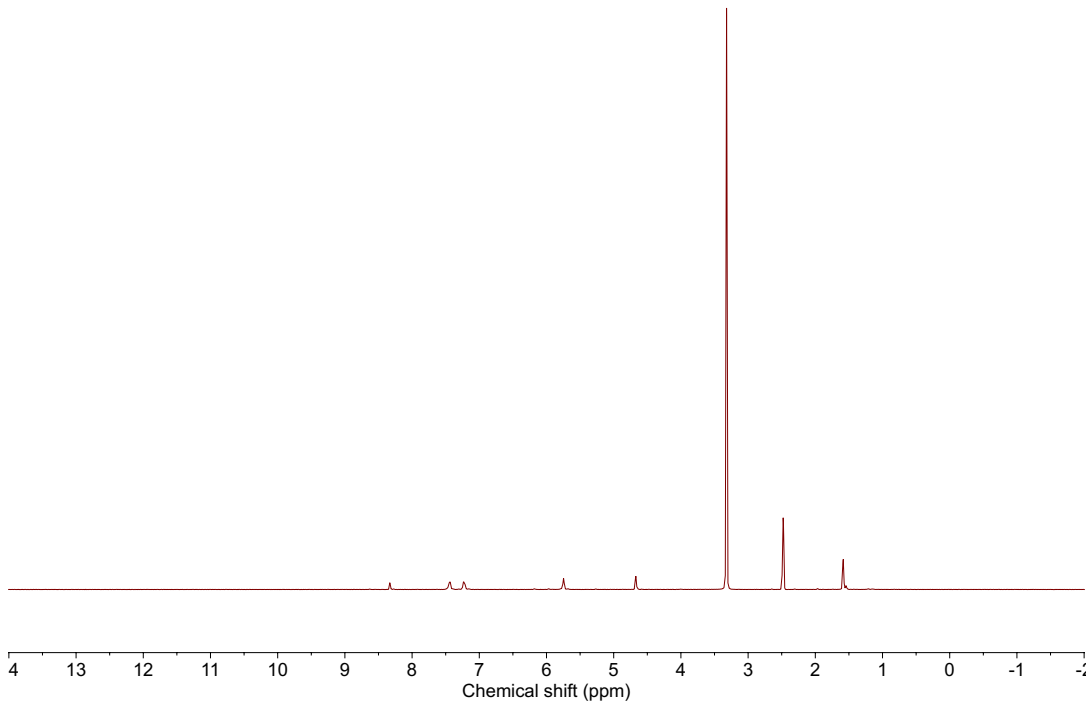

Fig. S9. ^{1}H NMR spectrum of compound **5** recorded in DMSO-d_6.

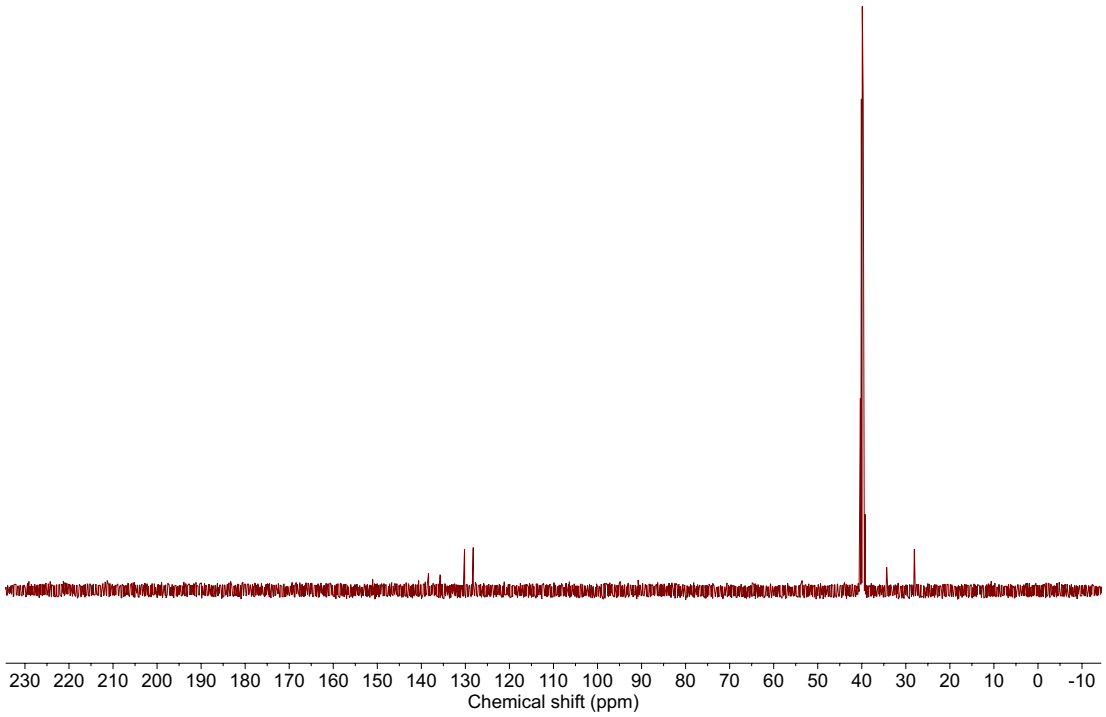

Fig. S10. ^{13}C NMR spectrum of compound **5** recorded in DMSO-d_6.

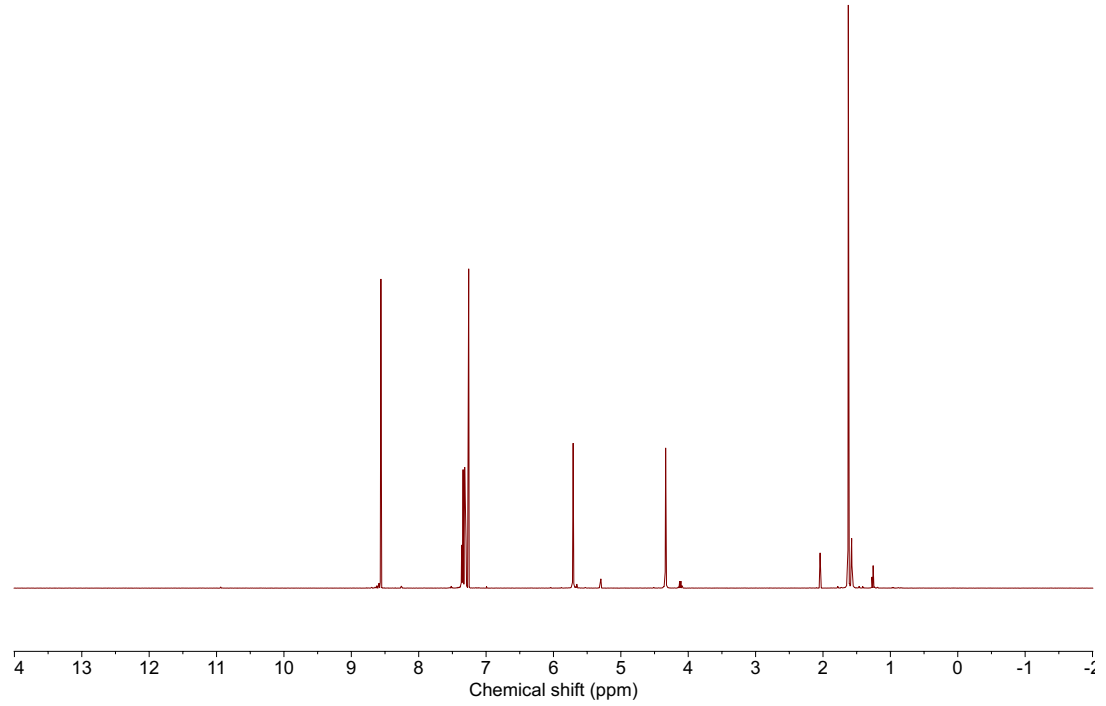

Fig. S11. ^{1}H NMR spectrum of compound **6** recorded in $CDCl_3$.

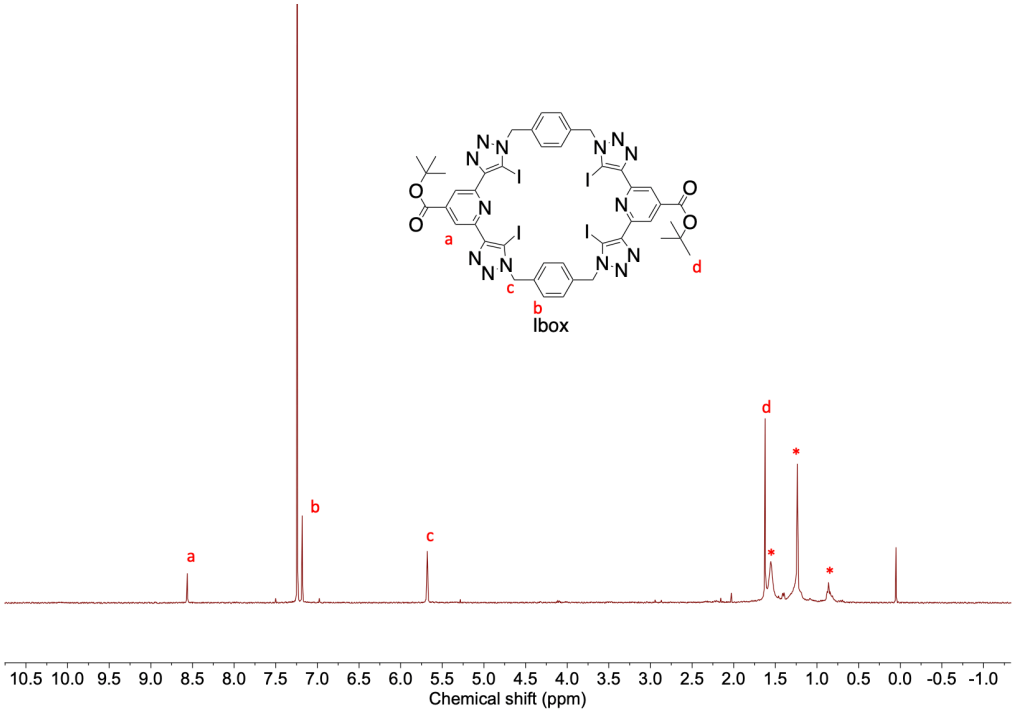

Fig. S12. ^{1}H NMR spectrum of the Ibox recorded in $CDCl_3$. The asterisks denotes residual solvent peaks.

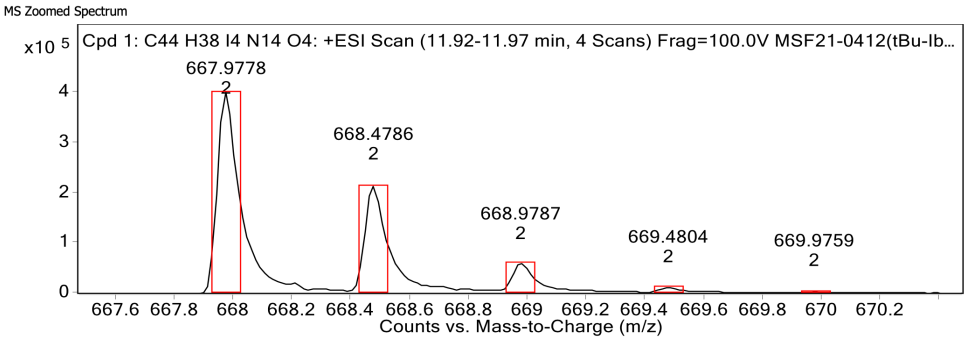

MS Spectrum Peak List

Obs. m/z	Calc. m/z	Charge	Abundance	Formula	Ion Species	Tgt Mass Error (ppm)
667.9778	667.9762	2	400899	C44H38I4N14O4	(M+2H)+2	-2.37
668.4786	668.4776	2	213909	C44H38I4N14O4	(M+2H)+2	-1.53
668.9787	668.9790	2	55305	C44H38I4N14O4	(M+2H)+2	0.34
669.4804	669.4803	2	9123	C44H38I4N14O4	(M+2H)+2	-0.12
669.9759	669.9816	2	1609	C44H38I4N14O4	(M+2H)+2	8.4
670.4810	670.4828	2	298	C44H38I4N14O4	(M+2H)+2	2.76
670.9066	670.9841	2	366	C44H38I4N14O4	(M+2H)+2	115.53
1356.9285			1481961			

--- End Of Report ---

Fig. S13. HR-ESI mass spectrum of the Ibox.

3. ^{1}H NMR titration data

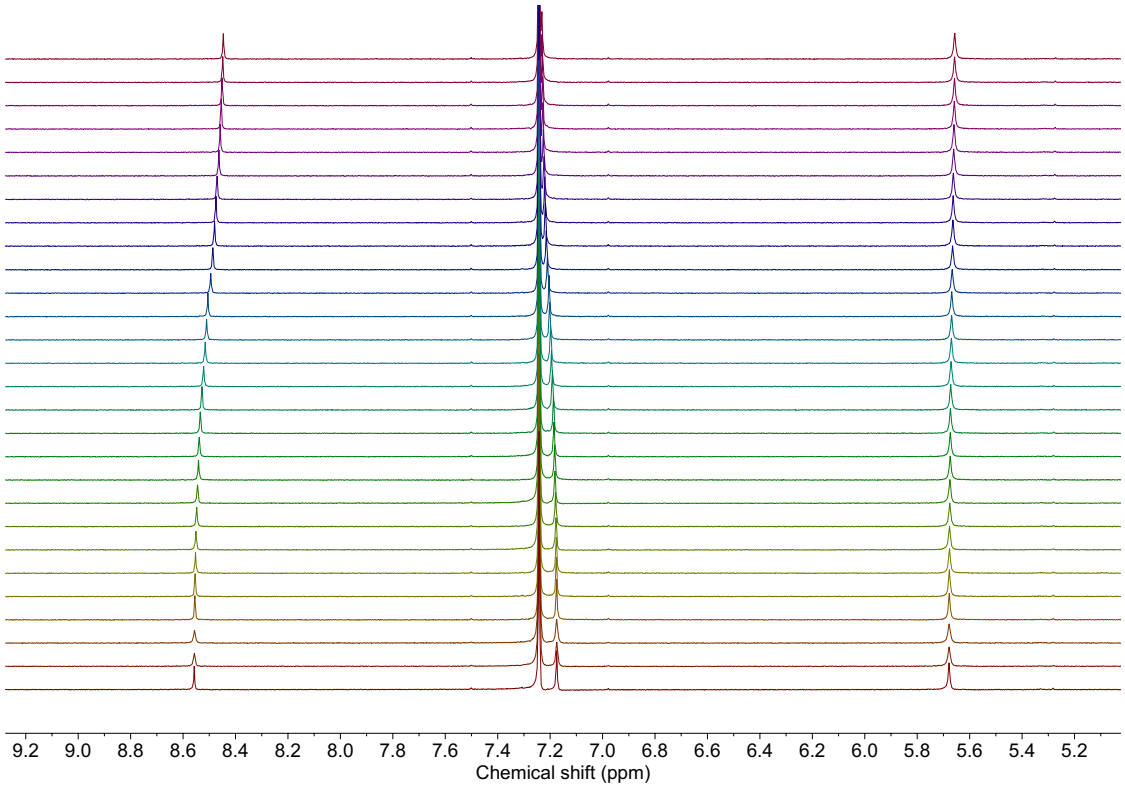

Fig. S14. Selected region of the ^{1}H NMR spectra ($CDCl_3$, 298 K) acquired during the titration of Ibox with increasing quantities of TBACl: 0, 0.20, 0.39, 0.58, 0.77, 0.95, 1.13, 1.48, 1.82, 2.14, 2.46, 2.76, 3.33, 3.87, 4.38, 4.85, 5.29, 6.30, 7.18, 7.95, 8.64, 9.24, 10.29, 11.15, 11.87, 12.48, 13.00 and 13.46 equiv. from bottom to top.

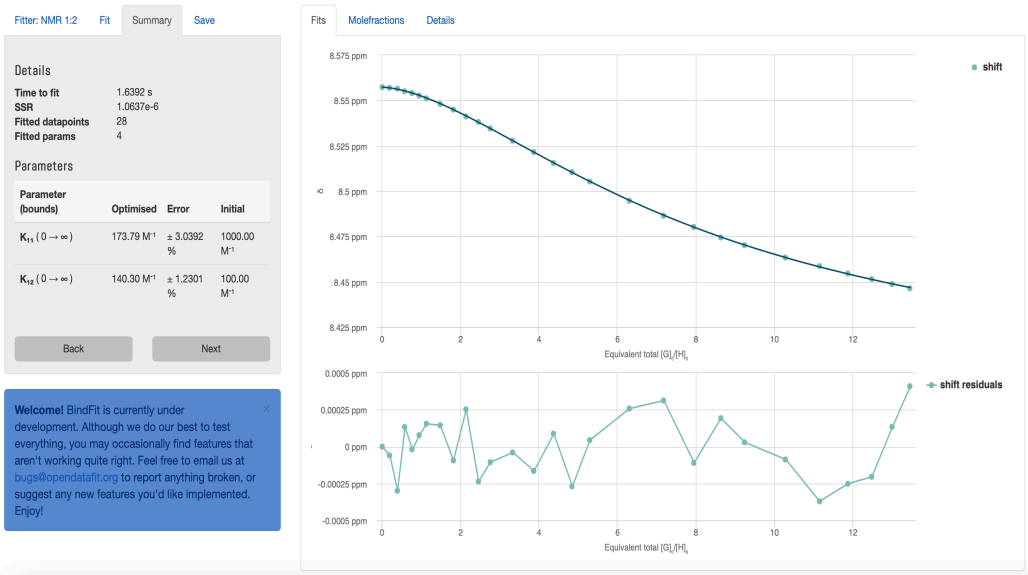

Fig. S15. Nonlinear least-square analysis of the ^{1}H NMR binding data corresponding to the formation of [Ibox•2Cl]$^{2-}$ using the BindFit web applet.[S4] The data were fitted to a 1:2 binding model to give K_{11} = (173 ± 5.3) and K_{12} = (140 ± 1.7). The residual distribution is shown below the binding isotherm.

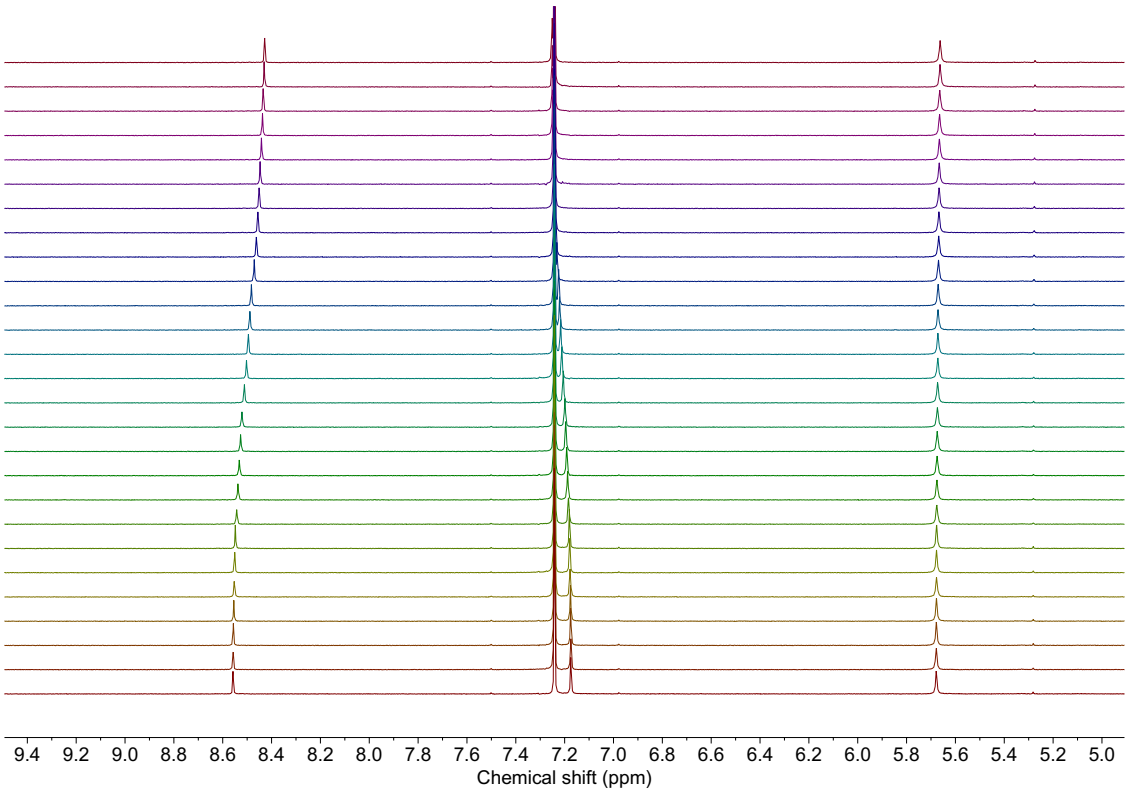

Fig. S16. Selected region of the ^{1}H NMR spectra ($CDCl_3$, 298 K) acquired during the titration of Ibox with increasing quantities of TBABr: 0, 0.20, 0.39, 0.58, 0.77, 0.95, 1.13, 1.48, 1.82, 2.14, 2.46, 2.76, 3.33, 3.87, 4.38, 4.85, 5.29, 6.30, 7.18, 7.95, 8.64, 9.24, 10.29, 11.15, 11.87, 12.48, 13.00 and 13.46 equiv. from bottom to top.

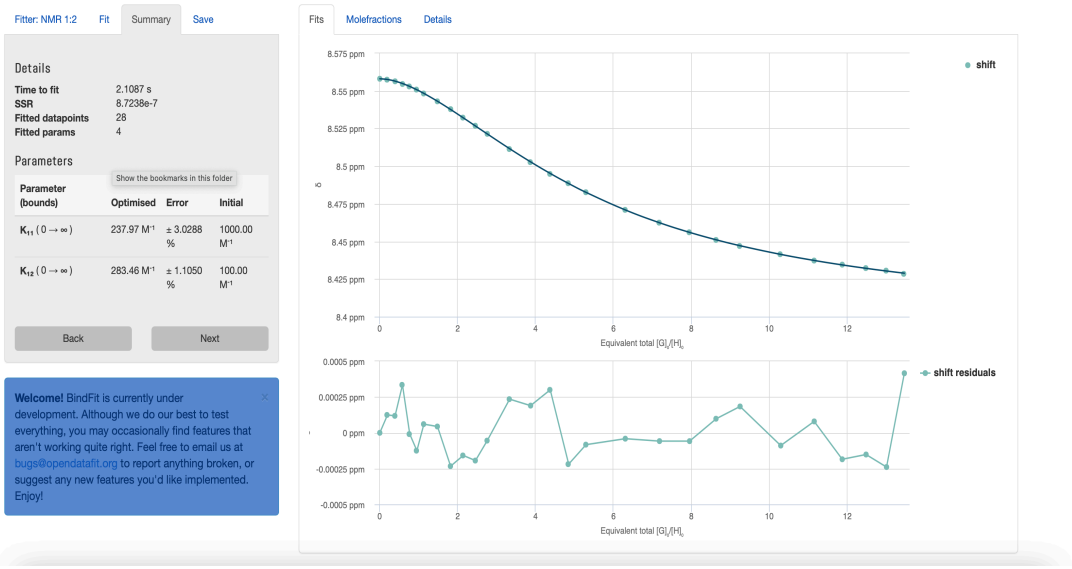

Fig. S17. Nonlinear least-square analysis of the ^{1}H NMR binding data corresponding to the formation of [Ibox•2Br]$^{2-}$ using the BindFit web applet. The data were fitted to a 1:2 binding model to give K_{11} = (238 ± 7.2) and K_{12} = (283 ± 3.1). The residual distribution is shown below the binding isotherm.

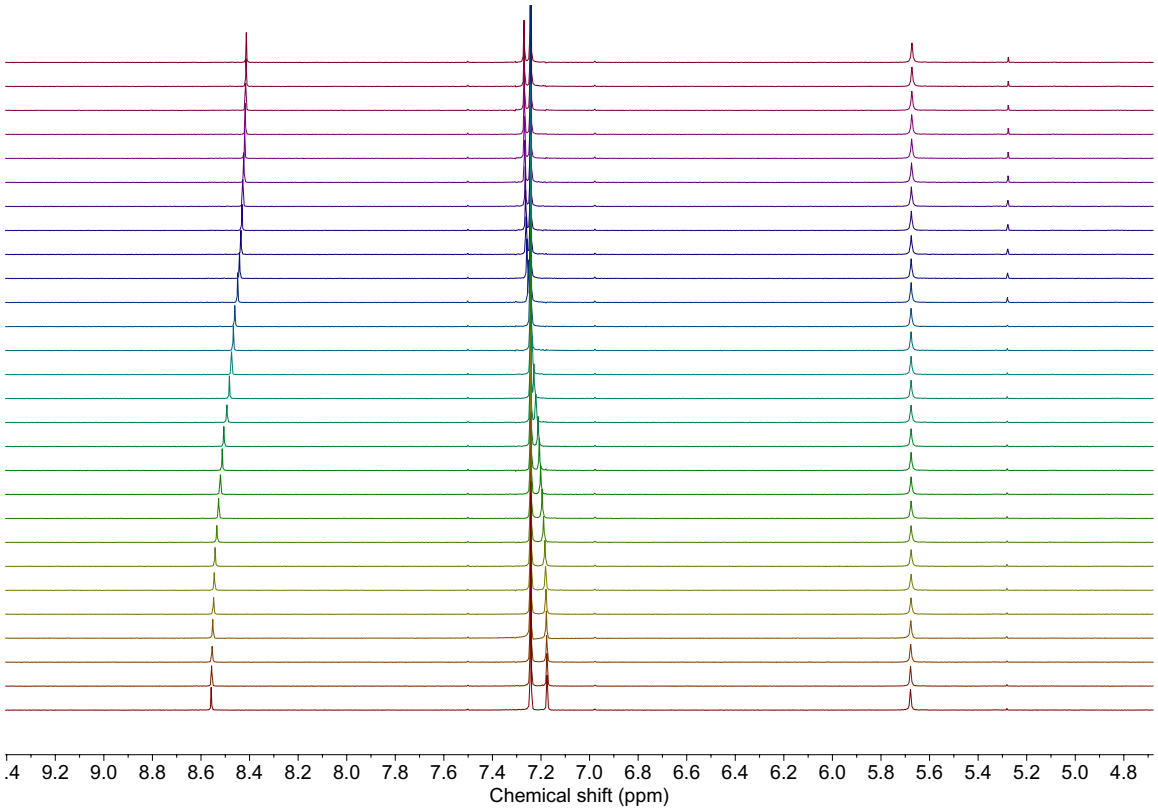

Fig. S18. Selected region of ^{1}H NMR spectra ($CDCl_3$, 298 K) acquired during the titration of Ibox with increasing quantities of TBAI: 0, 0.20, 0.39, 0.58, 0.77, 0.95, 1.13, 1.48, 1.82, 2.14, 2.46, 2.76, 3.33, 3.87, 4.38, 4.85, 5.29, 6.30, 7.18, 7.95, 8.64, 9.24, 10.29, 11.15, 11.87, 12.48, 13.00 and 13.46 equiv. from bottom to top.

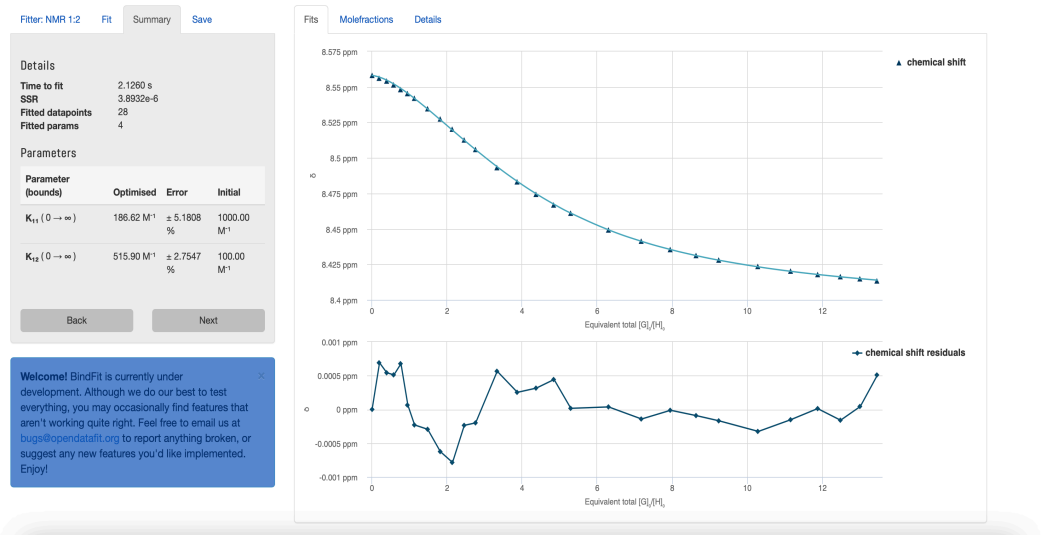

Fig. S19. Nonlinear least-square analysis of the ^{1}H NMR binding data corresponding to the formation of $[Ibox•2I]^{2-}$ using the BindFit web applet. The data were fitted to a 1:2 binding model to give $K_{11} = (187 \pm 9.7)$ and $K_{12} = (516 \pm 14)$. The residual distribution is shown below the binding isotherm.

4. Supporting X-ray experimental details

X-ray Experimental for $2C_{44}H_{38}N_{14}O_4I_4$ - $CHCl_3$: Crystals grew as colorless plates by vapor diffusion of hexane into a chloroform solution. The data crystal was cut from a larger crystal and had approximate dimensions; 0.16 x 0.047 x 0.044 mm. The data were collected on an Rigaku Oxford Diffraction SuperNova Dual Source diffractometer using a μ-focus Cu Kα radiation source (λ = 1.5418 Å) with collimating mirror monochromators. A total of 3146 frames of data were collected using ω-scans with a scan range of 1° and a counting time of 6 seconds per frame for frames collected with a detector offset of -41.6° and 24 seconds per frame with frames collected with a detector offset of 107.1°. The data were collected at 100 K using an Oxford Cryostream low temperature device. Details of crystal data, data collection and structure refinement are listed in Table 1. Data collection, unit cell refinement and data reduction were performed using Rigaku Oxford Diffraction's CrysAlisPro V 1.171.41.120a.[S5] The structure was solved by direct methods using SHELXT[S6] and refined by full-matrix least-squares on F^2 with anisotropic displacement parameters for the non-H atoms using SHELXL-2018/3.[S7] Structure analysis was aided by use of the programs PLATON[S8], OLEX2[S9]. The hydrogen atoms were calculated in ideal positions with isotropic displacement parameters set to 1.2xUeq of the attached atom (1.5xUeq for methyl hydrogen atoms).

There are two macrocycles in the asymmetric unit. Each lies around a different crystallographic inversion center. The phenyl rings were disordered in both. In one macrocycle, the *t*-butyl groups were disordered. The disorder was modeled using features available in OLEX2. A large region of disordered solvent was observed in the unit cell. The solvent mix could not be satisfactorily modeled. The contributions to the scattering factors due to these solvent molecules were removed by using SQUEEZE[S10].

The function, $\Sigma w(|F_o|^2 - |F_c|^2)^2$, was minimized, where $w = 1/[(\sigma (F_o))^2 + (0.2*P)^2]$ and $P = (|F_o|^2 + 2|F_c|^2)/3$. $R_W(F^2)$ refined to 0.225, with R(F) equal to 0.0720 and a goodness of fit, S, = 0.880. Definitions used for calculating R(F), $R_W(F^2)$ and the goodness of fit, S, are given below.[S11] The data were checked for secondary extinction effects but no correction was

necessary. Neutral atom scattering factors and values used to calculate the linear absorption coefficient are from the International Tables for X-ray Crystallography (1992).[S12] All figures were generated using SHELXTL/PC.[S13] Tables of positional and thermal parameters, bond lengths and angles, torsion angles and figures are found in the cif files that may be obtained from the Cambridge Crystallographic Data Centre upon request by quoting no. 2126348.

Table S1. Crystal data and structure refinement for 2Ibox·$CHCl_3$.

Empirical formula	C45 H39 Cl3 I4 N14 O4	
Formula weight	1453.85	
Temperature	100.02(14) K	
Wavelength	1.54184 Å	
Crystal system	triclinic	
Space group	P -1	
Unit cell dimensions	a = 13.4032(3) Å	α = 97.062(2)°.
	b = 13.4811(6) Å	β = 100.4278(18)°.
	c = 19.0017(3) Å	γ = 115.900(3)°.
Volume	2957.28(17) $Å^3$	
Z	2	
Density (calculated)	1.633 Mg/m^3	
Absorption coefficient	18.208 mm^{-1}	
F(000)	1404	
Crystal size	0.252 x 0.135 x 0.057 mm^3	
Theta range for data collection	2.428 to 73.796°.	
Index ranges	-16<=h<=14, -16<=k<=16, -23<=l<=23	
Reflections collected	48255	
Independent reflections	11564 [R(int) = 0.1067]	
Completeness to theta = 67.684°	99.5 %	
Absorption correction	Semi-empirical from equivalents	
Max. and min. transmission	1.000 and 0.45264	
Refinement method	Full-matrix least-squares on F^2	
Data / restraints / parameters	11564 / 897 / 785	
Goodness-of-fit on F^2	0.908	
Final R indices [I>2sigma(I)]	R1 = 0.0720, wR2 = 0.2102	

R indices (all data)	R1 = 0.0788, wR2 = 0.2250
Extinction coefficient	n/a
Largest diff. peak and hole	3.934 and -1.952 e.Å^{-3}
CCDC deposition number	2126348

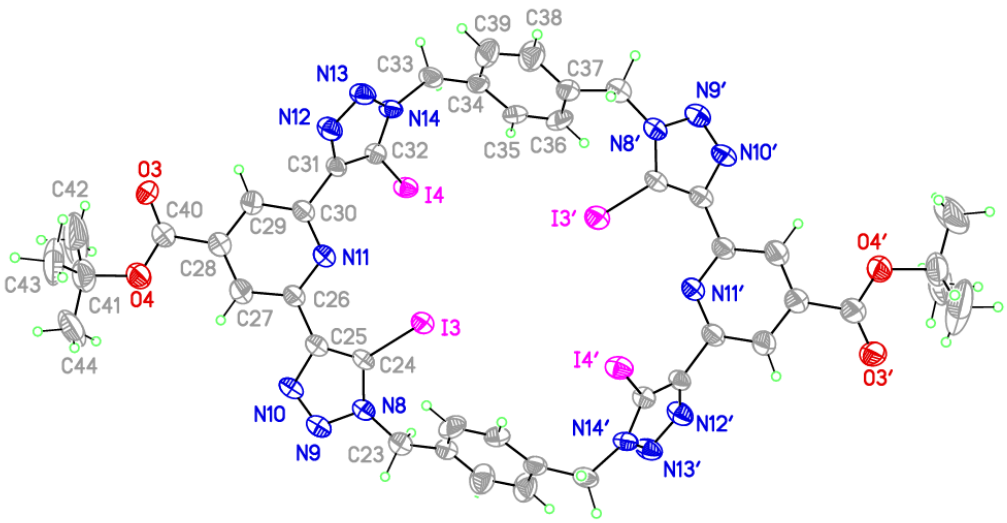

Fig. S20. View of the macrocycle 1 in Ibox showing the atom labeling scheme. Displacement ellipsoids are scaled to the 50% probability level. The lower occupancy atoms of the disordered phenol ring groups were omitted. The macrocycle resides around a crystallographic inversion center at 1, ½, 1. Atoms with labels appended by a ‘ are related by 2-x, 1-y, 2-z.

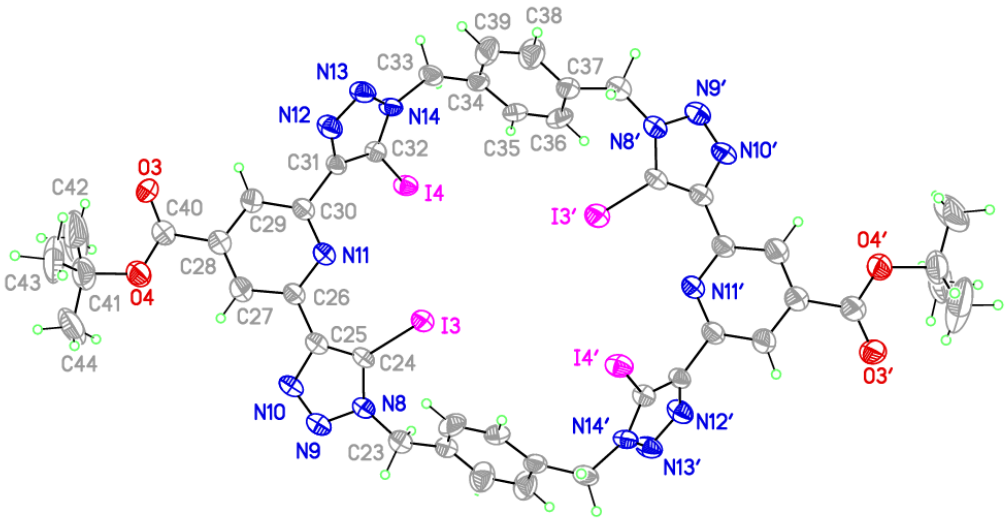

Fig. S21. View of the macrocycle 2 in **1** showing the atom labeling scheme. Displacement ellipsoids are scaled to the 50% probability level. The lower occupancy atoms of the disordered phenol ring groups were omitted. The macrocycle resides around a crystallographic inversion center at ½, 0, 1. Atoms with labels appended by a ‘ are related by 1-x, -y, 2-z.

References

S1. B. S. Gelinas, J. A. Jaye, G. R. Mattos and E. H. Fort, *Tetrahedron Lett*, 2015, **56**, 4232-4233.

S2. I. Abdelhedi-Miladi, D. Montarnal, M. M. Obadia, H. Ben Romdhane and E. Drockenmuller, *Acs Macro Lett*, 2014, **3**, 1187-1190.

S3. A. Borissov, I. Marques, J. Y. C. Lim, V. Felix, M. D. Smith and P. D. Beer, *J Am Chem Soc*, 2019, **141**, 4119-4129.

S4. BindFit. www.supramolecular.org

S5. CrysAlisPro. Rigaku Oxford Diffraction (2021). CrysAlisPro Software System, 1.171.41.120a.

S6. G. M. Sheldrick, SHELXT. A program for crystal structure solution. *Acta Cryst*. 2015, **A71**, 3-8.

S7. G. M. Sheldrick, SHELXL-2018/3. Program for the Refinement of Crystal Structures. *Acta Cryst*., 2015, **C71**, 3-8.

S8. A. L. Spek, PLATON, A Multipurpose Crystallographic Tool. Utrecht University, The Netherlands. *Acta Cryst*. 2009, **D65**, 148-155.

S9. O. V. Dolomanov, L. J. Bourhis, R. J. Gildea, J. A. K. Howard and H. Puschmann, OLEX2. A Complete Structure Solution, Refinement and Analysis Program. *J. Appl. Cryst*. **42**, 339-341.

S10. A. L. Spek, SQUEEZE. *Acta Cryst*. 2015, **C71**, 9-18.

S11. $R_W(F^2) = \{\Sigma w(|F_O|^2 - |F_C|^2)^2/\Sigma w(|F_O|)^4\}^{1/2}$ where w is the weight given each reflection.
$R(F) = \Sigma(|F_O| - |F_C|)/\Sigma|F_O|\}$ for reflections with $F_O > 4(\sigma(F_O))$.
$S = [\Sigma w(|F_O|^2 - |F_C|^2)^2/(n - p)]^{1/2}$, where n is the number of reflections and p is the number of refined parameters.

S12. International Tables for X-ray Crystallography (1992). Vol. C, Tables 4.2.6.8 and 6.1.1.4, A. J. C. Wilson, editor, Boston: Kluwer Academic Press.

S13. Sheldrick, G. M. (1994). SHELXTL/PC (Version 5.03). Siemens Analytical X-ray Instruments, Inc., Madison, Wisconsin, USA.